Clinical Kidney Journal

ckj

OXFORD

Leading European Nephrology

Clinical Kidney Journal, 2018, vol. 11, no. 2, 222–229

doi: 10.1093/ckj/sfx069
Advance Access Publication Date: 27 July 2017
Original Article

ORIGINAL ARTICLE

Metabolic adaptability in hexavalent chromium-treated renal tissue: an *in vivo* study

Kanu Shil and Sudipta Pal

Nutritional Biochemistry and Toxicology Laboratory, Department of Human Physiology, Tripura University, Suryamaninagar, West Tripura, India

Correspondence and offprint requests to: Sudipta Pal; E-mail: sudiptapal@tripurauniv.in

Abstract

Background: Hexavalent chromium [Cr(VI)], an environmental pollutant that originates mostly from anthropogenic sources, is a serious threat to human health. After entering into cells, Cr(VI) is capable of producing excessive free radicals and causing tissue damage. The present study aims to reveal the toxic manifestation of Cr(VI) on the metabolic activity of renal tissue.

Methods: Male Swiss albino mice were treated orally with potassium dichromate ($K_2Cr_2O_7$) at a dose of 10 mg/kg body weight for a period of 30 days. Important tricarboxylic acid (TCA) cycle enzyme activities like isocitrate dehydrogenase, succinate dehydrogenase and malate dehydrogenase, as well as the activities of enzymes involved in oxidative phosphorylation such as Nicotinamide adenine dinucleotide (NADH) dehydrogenase, were measured. Additionally, transaminase and protease (pronase, cathepsin and trypsin) activities, tissue protein and free amino nitrogen were estimated in renal tissue. Glucose-6-phosphatase, glucose-6-phosphate dehydrogenase and alkaline phosphatase activities, as well as lactic acid, pyruvic acid and chromium contents, of kidneys were determined following standard protocols. Kidney histology was performed by hematoxylin and eosin staining.

Results: Cr(VI) suppresses the rate-limiting enzymes of the TCA cycle and oxidative phosphorylation indicating an inhibition of renal ATP production. It decreases protease activity by eliminating the protein substrates and alters the gluconeogenic pathway. Cr(VI) worsens the normophysiological attributes of renal tissue by enhancing the activity of alkaline phosphatase, pointing towards kidney disease. Histopathological observations confirmed these biochemical results through the presence of chronic tubular nephritis and altered glomerular structure. Cr(VI) retention occurs to a greater extent in renal tissue, which intensifies the toxic manifestation of this pollutant in the kidney.

Conclusions: Cr(VI) disrupts the metabolic interaction between carbohydrates and proteins in mammalian renal tissue.

Key words: hexavalent chromium, oxidative phosphorylation, proteolytic enzymes, renal tissue, TCA cycle

Introduction

Heavy metal toxicity is a serious threat to living creatures across the globe. Overpopulation, rapid urbanization, excessive burning of fossil fuels, greedy industrialization and exhaustive opencast mining are anthropogenic activities that lead to pollution caused by heavy metals, including chromium. Chromium is an abundant trace element in the Earth's crust and exists in the environment at different valance states, ranging from hexavalent (VI) to trivalent (III) forms [1]. The former easily

Received: April 10, 2017; **Editorial decision:** May 30, 2017

accumulates in cells and causes irreversible toxic damage to their cellular conformation resulting in devastating effects on the surrounding tissue [2]. The diffusible form of chromium [hexavalent chromium, Cr(VI)] accumulates in various tissues of the exposed organism and forms an executive pattern of cellular toxicity that includes the disruption of normal morphophysiological cellular integrity. As a consequence, biochemical and enzymological functions related to metabolic processes are seriously disturbed [3]. India is the third most important exporter of chromium ore worldwide, contributing 19% of the total amount produced globally, of which 99% is mined from Odisha with the rest coming from other open-cast chromium mines [4, 5]. Cr(VI) leaches into water bodies and penetrates to ground water level, causing health complications among nearby inhabitants that range from chronic skin complaints to malignant cancer [6]. Cr(VI), being a potent oxidative stress modulator and apoptotic signal enhancer in renal tissue, has been shown to cause significant acute renal damage and advanced tubular necrosis in mammalian animal model systems [7]. The genotoxicity of Cr(VI) is evident as an excessive amount of free radicals and the production of DNA crosslinking, DNA–protein crossbinding, chromosomal aberrations and genomic instability in the nuclear environment of affected cells [8].

Although some functional aspects of the kidney's response to toxic insult have been well studied, to our knowledge there are no reports to date on protein and carbohydrate bioenergetics in renal tissue following exposure to chromium. The present study aims to identify the specific mechanism of the metabolic interactions of Cr(VI) in renal tissue with respect to protein and carbohydrate bioenergetics.

Materials and methods

Chemicals

Potassium dichromate ($K_2Cr_2O_7$, molecular weight 294.185), and chemicals including sodium succinate, triethanolamine, sodium citrate, sucrose, diethylether, bovine serum albumin (BSA), potassium hydroxide, ethanol, sulphuric acid (H_2SO_4), phenol, Tris-HCl, dichlorophenolindophenol (DCPIP) and ethylenediaminetetraacetic acid (EDTA) were of analytical grade and bought from Merck (Kolkata, India), SRL (Kolkata, India) and Sigma-Aldrich (Kolkata, India). All reagents were prepared using ultra-pure Millipore water to prevent unwanted metal contamination and to maintain experimental standards.

Animals

Swiss albino male mice ($n = 6$, number of animals per group) weighing 30–35 g were procured from Chakraborty Enterprise, Kolkata, India, an authorized animal supplier (Reg. No. 1443/PO/b/11/CPCSEA) nominated by the Control and Supervision of Experiments on Animals, Ministry of Environment and Forests, Govt of India. All procedures for animal maintenance, treatment and experimentation were in accordance with the ethical standards of the Institutional Animal Ethical Committee, Tripura University and were approved by the committee (Ref. No. TU/IAEC/2015/XI/2-3). Animals were housed in polypropylene cages and acclimatized to laboratory conditions for 1 week prior to the start of the experiment. Animals were provided with a standard protein diet (18% casein diet) and supplied with drinking water *ad libitum* throughout the experiment. The animal house maintained standard air conditions of temperature (22–25°C) with a 12 h alternating light and dark cycle.

Experimental design

Animals were divided into two groups of equal average body weight: the control and Cr(VI)-treated groups. Each group consisted of six animals ($n = 6$) that were subjected to the following treatment protocols.

Control group: animals received Millipore water orally.

Cr(VI)-treated group: animals were treated with Cr(VI) (as $K_2Cr_2O_7$) at a dose of 10 mg/kg body weight/day orally for 30 days.

Animal sacrifice

After the treatment period, all animals were sacrificed by cervical dislocation following the guidelines of the Institutional Animal Ethical Committee.

Separation of tissue

Subsequent to animal sacrifice, kidneys were removed from all animals, washed in ice-cold saline (0.9%), blotted dry, weighed and kept at −20°C for biochemical analyses.

Preparation of tissue homogenate

Tissue homogenates were prepared in suitable buffer solution (e.g. 0.1 M phosphate buffer, pH 7.4 and 0.25 M sucrose solution) as required for different analytical methods using a Potter Elvenjem glass homogenizer (Belco Glass Inc., Vineland, NJ, USA).

Preparation of mitochondrial suspension from renal tissue

Kidney tissue mitochondria were isolated according to the method of Dutta *et al.* [9]. A portion of the kidney was cleaned and cut into small pieces. Next, 500 mg of the tissue was incubated with 10 mL sucrose buffer solution [0.25 M sucrose, 0.001 M EDTA and 0.05 M Tris-HCl (pH 7.8)] at 25°C for 5 min. The tissue was then homogenized in a cold environment for 1 min at low speed using a Potter Elvenjem glass homogenizer. The homogenate was centrifuged at 1500 rpm for 10 min at 4°C and the resulting supernatant centrifuged at 4000 rpm for 5 min at 4°C. The supernatant, thus obtained, was further centrifuged at 14 000 rpm for 20 min at 4°C. The final supernatant was discarded and the pellet was resuspended in sucrose buffer. Most of the enzymatic assays were carried out with freshly prepared mitochondrial suspension, but suspensions were stored at − 20°C until further analysis if necessary.

Body weight and kidney-somatic index

The body weight of each animal of each group was recorded on the day that treatment commenced and was also noted periodically until sacrifice to observe the changes in body weight in different groups. The organ weights (both kidneys) of the animals were also recorded after sacrifice. The kidney-somatic index (KSI) was calculated according to the following formula of Krishnaiah and Reddy [10].

$$\mathrm{KSI} = \frac{\text{Weight of the organ (g)}}{\text{Day 30th total body weight}} \times 100$$

Pyruvic acid content

The pyruvic acid content of kidney tissue was estimated according to the protocol of Segal *et al.* [11]. Briefly, 10% tissue

homogenate was centrifuged at 3000 rpm for 10 min with 5% tricarboxylic acid (TCA). The resulting supernatant was mixed with 1 mL distilled water and 0.5 mL 2,4 Dinitrophenylhydrazine (DNPH) and shaken for 3 min. Then, toluene was added and mixed vigorously by hand shaking for a few minutes. After that, 2 mL each of sodium carbonate and NaOH solution was added to measure the optical density of the colored product at 420 nm. The observed result was expressed as μg/g of tissue.

Lactic acid content

Lactic acid content of the kidney tissue was determined by the colorimetric method of Taylor [12]. In brief, a 0.5 mL tissue aliquot was placed in a screw-capped borosilicate tube with 3 mL of concentrated H_2SO_4, heated to boiling temperature for 10 min and then cooled in a water bath. After that, 50 μl 4% $CuSO_4$ and 100 μl of 1.5% p-phenylphenol (prepared with ethanol) were added one after another, mixed thoroughly and the tube was incubated for 30 min at 30°C until all of the precipitate had dissolved. The absorbance was measured at 570 nm and the result expressed in terms of mg/g of tissue.

Lactate dehydrogenase activity

Lactate dehydrogenase (LDH) activity was estimated via the method of Bergmeyer [13], which measures the activity of the enzyme by the rate of consumption of pyruvate and reduced Diphospho pyridine nucleotide (DPNH) in the tissue homogenate. Decreased optical density at 340 nm was measured in an UV-vis spectrophotometer for oxidation of DPNH at 10 s intervals for 5 min. Enzyme activity was expressed as unit/min/mg of protein.

Pyruvate dehydrogenase activity

Pyruvate dehydrogenase activity was measured via the method of Liu and Bisswanger [14]. The required assay mixture for enzyme estimation contained triethanolamine buffer with 0.1 M $MgCl_2$, 0.1 M pyruvate, 0.01 M DCPIP at pH 7.8 and a specific amount of tissue homogenate. Kinetic changes were recorded at 597 nm and the results expressed as mmol/min/mg of protein.

Glucose-6-phosphatase activity

To measure Glucose-6-phosphatase (G6Pase) activity, 5% kidney tissue homogenate was mixed with 1.8 mL of buffer substrate, then incubated at 37°C for 10 min. After incubation, 1 mL of ice-cold TCA was added and centrifuged at 3000 rpm for 10 min. The resulting supernatant was taken for the estimation of liberated inorganic phosphate. Optical density was measured at 880 nm according to the method of Plummer [15]. The activity of G6Pase was expressed as μg phosphate liberated/min/mg of protein.

Glucose-6-phosphate dehydrogenase activity

Glucose-6-phosphate dehydrogenase (G6PD) activity was measured via the technique of Bergmeyer [16]. For the determination of enzymatic activity, the assay mixture was prepared with 0.1 M triethnolamine, 0.1 M glucose-6-phosphate, 0.1 M $MgCl_2$ and 0.04 M NADH. Then, 0.98 mL of assay mixture was added to 0.02 mL tissue homogenate. The increase in absorbance was measured at 30 s intervals at 340 nm at 25°C for 5–8 min. Enzyme activity was expressed as mmol of NADH reduced/min/mg of protein.

Isocitrate dehydrogenase activity

Mitochondrial isocitrate dehydrogenase (IDH) activity was measured according to the method of King [17]. The reaction mixture contained 0.1 mL of Tris-HCl, 0.2 mL of trisodium isocitrate, 0.3 mL of manganese chloride, 0.2 mL of mitochondrial suspension and 0.2 mL of NADP (0.2 mL of saline for control). After incubation, 0.001 M of DNPH was added followed by the addition of 0.005 M of EDTA and 0.4 N NaOH. Optical density was taken at 420 nm in an UV-vis spectrophotometer. Enzyme activity was expressed as unit/min/μg of protein.

Succinate dehydrogenase activity

Succinate dehydrogenase (SDH) activity was measured spectrophotometrically in a mitochondrial suspension following the reduction of $K_3Fe(CN)_6$ at 420 nm according to the method of Dutta *et al.* [9]. Each 1 mL of assay mixture contained 50 mM phosphate buffer (pH 7.4), 2% (w/v) BSA, 4 mM succinate, 2.5 mM $K_3Fe(CN)_6$ and a suitable aliquot of the enzyme. Enzyme activity was expressed as unit/min/mg of protein.

Malate dehydrogenase activity

Malate dehydrogenase (MDH) activity in the mitochondrial suspension was determined via the method of Mehler *et al.* [18] using an assay mixture containing potassium phosphate buffer, 0.0076 M oxaloacetic acid and 0.005 M NADH at pH 7.4. The reduction of NADH was measured at 340 nm for 5 min a 10 s intervals and activity expressed as mmol of NADH oxidized/min/mg of protein.

NADH: ubiquinone C oxidoreductase (complex I) activity

The activity of NADH: ubiquinone C oxidoreductase was measured via the method of Minakami *et al.* [19]. The reaction mixture contained 1 mL phosphate buffer, 0.1 mL of potassium ferricyanide and 0.2 mL mitochondrial suspension in a total reaction volume of 3 mL with distilled water. Freshly prepared (0.1%) NADH solution was added just before the addition of the enzyme, except in the control set. The change in optical density was measured at 420 nm for 3 min and enzyme activity expressed as mmol of NADH oxidized/min/mg of protein.

Tissue protein content

Protein content was estimated according to the method of Lowry *et al.* [20]. First, 0.1 mL of tissue homogenate was mixed with 0.9 mL distilled water and 4.5 mL alkaline copper reagent and kept at room temperature for 10 min. To this, 0.5 mL of Folin's reagent (1:2) was added. The blue color was allowed to develop for 20 min and before optical density was read at 640 nm. Protein content was expressed as g/100 g tissue.

Free amino acid nitrogen content

The 5% tissue homogenate (in 0.1 M phosphate buffer, pH 7.4) was first dissolved in 0.67 (N) H_2SO_4 and 10% Na-tungstate to precipitate proteins, then centrifuged to obtain the protein-free extract. The resultant supernatant was treated with cyanide acetate buffer and 3% ninhydrin solution as per the protocol proposed by Rosen [21]. After that, the solution was heated at 100°C in a water bath for 5 min and isopropanol added immediately after cooling to enable the violet color to develop. Optical density of the colored solution was measured in a

spectrophotometer at 570 nm. Free amino nitrogen level was expressed as mg/g tissue.

Alkaline phosphatase activity

The alkaline phosphatase activity of renal tissue was determined via the method of Kind and King [22] using tissue homogenate prepared with 0.1 M phosphate buffer solution. At alkaline pH, this enzyme hydrolyses its substrate p-nitrophenyl phosphate and forms phenol, which further reacts with aminoantipyrine in the presence of ferricyanide to produce a colored derivative. The intensity of the colored derivative formed is directly proportional to the enzymatic activity in the tissue homogenate. Enzyme activity was expressed as King–Armstrong unit/mg of tissue.

Glutamate pyruvate transaminase and glutamate oxaloacetate transaminase activities

Transaminase enzyme activities in the studied tissue were determined following the method of Reitman and Frankel [23]. For this assay, a standard kit (Coral Clinical Systems, Goa, India) was used to photometrically measure the color intensity of the reaction mixture: color forms due to the chemical reaction of alanine with α-ketoglutarate to form pyruvate in the case of glutamate pyruvate transaminase (GPT), whereas aspartate reacts with α-ketoglutarate to form pyruvate in the case of glutamate oxaloacetate transaminase (GOT). Following the addition of the reagents, tubes were incubated at 37°C for a specific period of time and absorption noted at 505 nm. Enzyme activity was expressed in terms of unit/g of tissue.

Pronase activity

Pronase activity in kidney tissue was estimated following the method of Barman [24]. A 5% tissue homogenate in sucrose solution was incubated at 40°C temperature with casein substrate for 30 min. The reaction was stopped by addition of protein precipitating reagent solution. The mixture was then centrifuged, the supernatant collected and its optical density measured at 280 nm wavelength. Pronase activity was expressed as nmol of tyrosine produced/min/mg of protein.

Trypsin activity

To determine the activity of trypsin in 5% tissue homogenate, the method of Green and Work [25] was employed. In this method two separate tubes were taken, one containing a defined volume of tissue homogenate and 2.5 mL of Hemoglobin (Hb) substrate (the sample tube) and the other containing 5% TCA and Hb substrate (buffer blank). Both tubes were incubated at 25°C for 30 min, after which 5% TCA was added to the sample tube to stop the reaction and 5% tissue homogenate was added to the buffer blank. Tyrosine content was measured in a spectrophotometer at 280 nm wavelength. Enzyme activity was calculated as nmol of tyrosine produced/min/mg of protein.

Cathepsin activity

The activity of cathepsin in kidney tissue was assayed via the method of Pokrovsky *et al.* [26]. According to this procedure, 5% tissue homogenate was added to Hb substrate (4%) and incubated at 37°C for 1 h. To stop the reaction, 8% TCA was added and mixed well. In the same manner, a buffer blank was also prepared in which TCA was added before incubation with the same ingredients as were in the sample tube. After precipitation of protein in the mixture, the supernatant was collected by centrifugation at 3500 rpm for 10 min. Optical density was measured in a UV-vis spectrophotometer at 280 nm. Tissue cathepsin activity was expressed in terms of nmol of tyrosine produced/min/mg of protein.

Tissue Cr(VI) analysis

Tissue Cr(VI) content was determined using an atomic absorption spectrometer (Perkin Elmer A Analyst 700) according to the method suggested by Sun and Liang [27]. Data were collected from three pooled samples and expressed as μg/g of tissue.

Histopathological studies

For histopathological analysis of kidney samples, both control and Cr(VI)-treated tissues were preserved in 10% neutral buffered formalin solution for 24 h. After dehydration in graded alcohol, clearing, impregnation and embedding, tissue sections were prepared with a rotary microtome, stained using hematoxylin and eosin, and examined by microscopy. Photomicrographs were taken using a 20× objective.

Statistical analyses

All results were expressed as means ± standard error of the mean (SEM). Significance of differences between the two groups were assessed using a paired Student's *t*-test. $P < 0.05$ was considered statistically significant.

Results

Body weight: Sub-acute chromium exposure (represented in Table 1) at the dose and duration utilized in this study had no significant effect on the body weight of experimental mice.

KSI: Table 1 shows that chromium intoxication affected the organo-somatic index of kidneys in the treated group of mice as the KSI increased. In the treated group, KSI increased by 21.72% ($P < 0.05$) compared with the control group.

Total protein content: Table 2 demonstrates that kidney protein content decreased significantly (by 44.49%, $P < 0.001$) compared with the control group.

Free amino nitrogen content: The free amino nitrogen level was elevated fourfold with Cr(VI) intoxication ($P < 0.001$) as compared with the control group (Table 2).

Pyruvic acid content: Table 2 shows that Cr(VI) exposure resulted in a significant decrease in the pyruvic acid content of renal tissue (69%, $P < 0.05$).

Lactic acid content: Table 2 demonstrates that the observed increase (20%) in lactic acid content in renal tissue due to chromium exposure was not statistically significant ($P > 0.05$).

Tissue chromium deposition: Cr(VI) accumulation in renal tissue was found to be 2.58-fold compared with the control group (Table 2).

PDH activity: A significant decrease (40.42%, $P < 0.001$) in PDH activity was observed in the renal tissue of mice after chromium exposure (Table 3).

Alkaline phosphatase activity: Enzyme activity was significantly elevated in renal tissue by approximately twofold ($P < 0.001$) after sub-acute Cr(VI) exposure (Table 3).

NADH dehydrogenase (mitochondrial complex I) activity: As represented in Table 3, chromium intoxication significantly decreased NADH dehydrogenase activity in treated mice in

Clinical Kidney Journal
ckj

Table 1. Effect of sub-acute doses of Cr(VI) on body weight and KSI

Groups of animals ($n = 6$)	Final body weight (g) after 30 days	Kidney somatic index kidney weight × 100/body weight (g)
Control	36.75 ± 3.07	1.52 ± 0.04
Treated	34.29 ± 3.31; $P > 0.05$	1.85 ± 0.12; $P < 0.05$

Values are means ± SEM. $P < 0.05$ was considered as statistically significant.

Table 2. Effect of sub-acute exposure to Cr(VI) on different metabolic parameters in renal tissue

Metabolic parameters	Kidney tissue	
	Control	Treated
Total protein content (g/100 g of tissue) (6)	26.34 ± 1.32	14.62 ± 0.8; $P < 0.001$
Free amino nitrogen (mg/g of tissue) (6)	0.086 ± 0.007	0.38 ± 0.02; $P < 0.001$
Pyruvic acid content (μg/g of tissue) (6)	192.38 ± 6.36	59.48 ± 3.15; $P < 0.05$
Lactic acid (mg/g of tissue) (6)	15.26 ± 2.06	18.32 ± 2.72; $P > 0.05$
Chromium content (μg/g tissue) (3)	7.4	19.4

Values are means ± SEM, except the parameter of chromium content in tissue, which represents pooled data from three samples. Figures in parentheses indicate number of animals. $P < 0.05$ and $P < 0.001$ were considered statistically significant. $P > 0.05$ was not significant.

Table 3. Effect of sub-acute exposure to Cr(VI) in kidney on different enzyme activities

Metabolic enzymes	Kidney tissue	
	Control	Treated
PDH (unit/min/mg of protein) (6)	1.88 ± 0.10	1.12 ± 0.08; $P < 0.001$
Alkaline phosphatase (King–Armstrong unit/mg of tissue) (6)	0.64 ± 0.04	1.29 ± 0.08; $P < 0.001$
NADH dehydrogenase (mmol of NADH oxidized/min/mg of protein) (6)	6.78 ± 0.62	1.7 ± 0.39; $P < 0.001$
Pronase activity (nmol of tyrosine/min/mg of protein) (6)	1.38 ± 0.4	0.28 ± 0.09; $P < 0.001$
Cathepsin activity (nmol of tyrosine/min/mg of protein) (6)	1.03 ± 0.06	0.33 ± 0.07; $P < 0.001$
Trypsin activity (nmol of tyrosine/min/mg of protein) (6)	35.08 ± 3.2	13.04 ± 3.33; $P < 0.001$

Values are means ± SEM. Figures in parentheses indicate number of animals. $P < 0.05$ and $P < 0.001$ are considered statistically significant.

comparison with the control group. The percentage change observed was 74.92% ($P < 0.001$).

Protease activity: Table 3 shows that protease activity decreased in Cr(VI)-exposed renal tissue. Pronase, cathepsin and trypsin activity decreased by 79.72% ($P < 0.001$), 67.96% ($P < 0.001$) and 62.82.9% ($P < 0.001$), respectively.

IDH activity: Figure 1 shows that IDH activity in kidney tissue was decreased by 33.46% ($P < 0.001$) in the Cr(VI)-treated group.

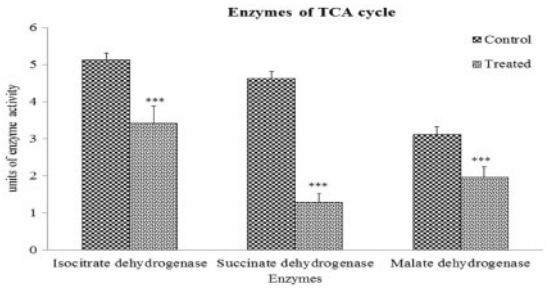

Fig.1. Altered TCA cycle enzyme activities due to hexavalent chromium exposure. Values are expressed as means ± SEM. Asterisks indicate significant difference relative to control (***$P < 0.001$). Number of animals in each group of experimental set was six.

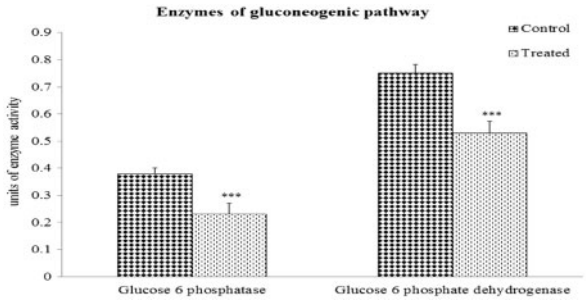

Fig. 2. Changes in gluconeogenic enzyme activities of kidney due to Cr(VI) toxicity. Values are expressed as means ± SEM. Asterisks indicate significant difference relative to control (***$P < 0.001$). Number of animals in each group of experimental set was six.

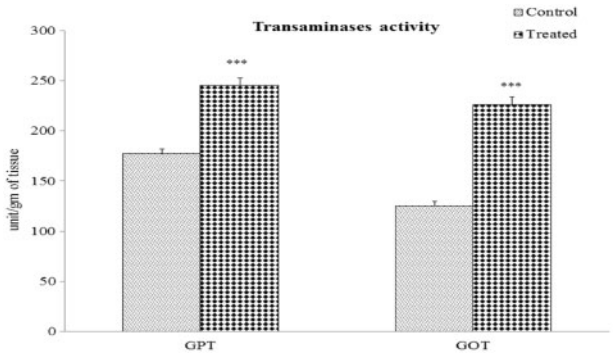

Fig. 3. Altered transaminase activities of the renal tissue after chromium exposure. Values are expressed as means ± SEM. Asterisks indicate significant difference relative to control (***$P < 0.001$). Number of animals in each group of experimental set was six.

SDH activity: The results presented in Figure 1 reveal that CR(VI) treatment significantly decreased SDH activity by 72.14% ($P < 0.001$) in mouse kidney tissue compared with the control group.

MDH activity: Figure 1 shows that MDH activity in kidneys of treated mice was significantly decreased (36.85%, $P < 0.001$) compared with that of the control group.

G6Pase activity: Figure 2 demonstrates that the activity of G6Pase in the renal tissue of Cr(VI)-exposed mice was decreased by 39% ($P < 0.001$) compared with that of the control group.

G6PD activity: Figure 2 shows that G6PD activity was decreased by 29.3% ($P < 0.001$) in mouse renal tissue after Cr(VI) exposure.

Transaminase activity: GPT activity was significantly increased by 38% ($P < 0.001$) and GOT activity was also elevated

by 80.38% ($P < 0.001$) in the kidneys of Cr(VI)-treated mice compared with their respective control groups (Figure 3).

LDH activity: LDH activity was significantly increased in the kidney tissue of Cr(VI)-treated mice (35.46%, $P < 0.001$) compared with that of the control group (Figure 4).

Histopathological micrographs of kidney tissue: Figure 5 shows representative histopathological micrographs of mouse kidney tissue. There was significant ectopic alteration in the structure of kidney tissue in Cr(VI)-treated mice, owing to drastic changes in glomerular attributes and tubular conformation.

Discussion

Metabolic perturbations in renal tissue following chromium exposure, including alterations in protein and carbohydrate bioenergetics, have been addressed in the present study. Exposure to chromium did not lead to a gain in body weight of treated mice, indicating that change in body weight is a factor that is independent of short-term chromium exposure. The slight increase in KSI observed in chromium-treated mice might be due to an excess accumulation of chromium in renal tissue or mild fat deposition. Heavy metals of the transition element group, such as Cr(VI), are potential generators of oxidative stress and endocrine-disrupting chemicals, which are able to disrupt a wide range of biochemical cascades in tissues ranging from hepatic to muscular tissue [28]. Toxicity-induced proliferative stress molecules exert an irreversible toxic effect on kidney tissue [29]. Cr(VI) exerts detrimental effects on the biological attributes of cells by interfering with the enzymatic processes of different metabolic systems. Cr(VI) is able to mimic the active cofactors of some enzymes and bind covalently to them, resulting in conformational alterations and the subsequent diminution of their activities [30]. Cr(VI) has also been shown to cause hepatocyte cytotoxicity and interstitial nephritis in experimental animals [31]. Being the most stable and easily diffusible chromium compound, Cr(VI) is readily deposited in cellular structures where it is intensely cytotoxic [32]. Overaccumulation of chromium in renal tissue was evident in the present study. Histopathological observations also confirmed retention of Cr(VI) in renal tissue with the effect of altered glomerular structure, severe necrosis and hyalinized cytoplasm, with structural defects visible in the distal and proximal convoluted tubules.

Cr(VI) is an eventual free radical generator and an effective disintegrator of sequential metabolic pathways in different tissues of exposed organisms [33]. It triggers significant kidney damage, cellular malfunction, proteinuria, glycosuria and defective renal reabsorption owing to severe nephrotoxicity [34]. Chromium's metabolic toxicity results from its effect on glycolytic activity, evidenced by the suppressed production of pyruvate and decreased activity of PDH in renal tissue, which may contribute to disturbance of the metabolic link between the glycolytic pathway and the TCA cycle, thus hampering energy production. In the present study, the apparent decrease in pyruvate in renal tissue due to decreased PDH and increased LDH activity is not in accordance with the usual mechanism. It is likely that the increased activity of transaminase may lead to the conversion of pyruvate to alanine, decreasing the level of pyruvate in renal tissue after chromium exposure. Such pyruvate depletion in renal tissue is evident in acute kidney diseases, [35]. Additionally, in renal complications such as acute and chronic kidney diseases, pyruvate passes out from renal tissue and either accumulates in the blood or is excreted in the urine [36]. As Cr(VI) facilitates the perturbation of important biochemical intermediates by toxic manifestation of defensive antioxidant molecules of the cell, it consequently creates an environment inside the cell that is unfavorable for the execution of metabolic functions [31, 37]. This may cause renal disorders such as acute kidney disease, which implies severe nephron cell damage and functional dysregulation in the renal tissue [38].

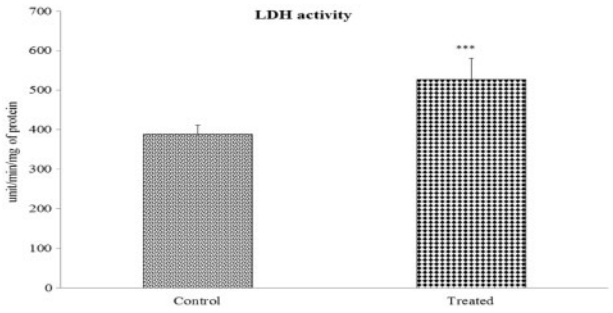

Fig. 4. Effect of Cr(VI) on renal LDH activity. Values are expressed as means ± SEM. Asterisks indicate significant difference relative to control (***$P < 0.001$). Number of animals was six in each group of experimental set.

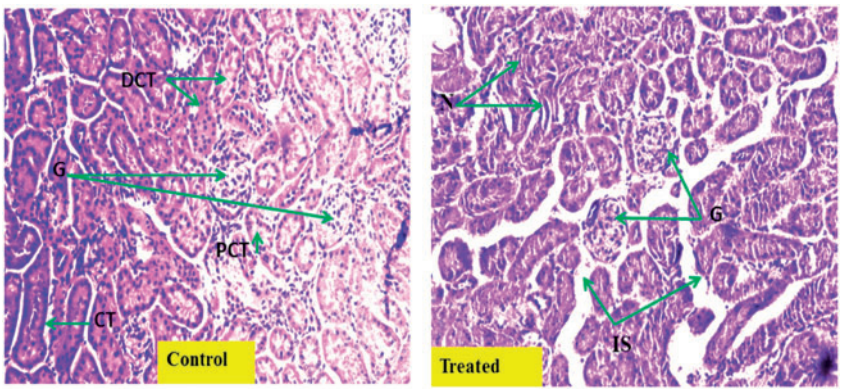

Fig. 5. Histopathological changes in kidney tissue after Cr(VI) exposure. Representative hematoxylin and eosin-stained histological sections from kidney of vehicle-treated normal renal cortex (Control) (magnification 20×; G, glomerulus; PCT, proximal convoluted tubule; DCT, distal convoluted tubule; CT, collecting tubule); and (Treated) chromium-treated mice renal cortex [magnification 20×: tubular damage with mild tubular dilatation, necrosis of tubular epithelial cells (N) and increased interstitial spaces (IS)].

In our study, all of the key enzymes of the TCA cycle were affected in the renal tissue of the Cr(VI)-exposed group. The significant reduction in the activities of IDH and MDH resulted in disruption of the TCA cycle and diminished ATP production. Our findings are supported by a recent study that observed that the metabolic toxicity of Cr(VI) is partly due to its hampering of ATP production [39]. Cr(VI) affects the NADH production as well as disrupting general metabolic processes by interfering with the production of intermediate metabolic byproducts. Additionally, Cr(VI) exposure significantly reduces SDH activity in renal tissue, where it has a retrogressive effect on metabolic cycles of energy production and hampers normal physiological functions, which may lead to chronic nephritis. In the present study, NADH dehydrogenase activity was found to be decreased in the renal tissue after sub-acute chromium exposure indicating disturbed function of the mitochondrial electron transport chain leading to reduced energy production. The ability of Cr(VI) to suppress mitochondrial enzymes and ATP production has been noted by previous studies [39, 40].

Cr(VI) exposure can have detrimental effects on the activities of gluconeogenic enzymes by combining with them in a way that disrupts their normal conformation [41]. In the present study, Cr(VI) downregulated the activities of two important enzymes of the gluconeogenic pathway, G6Pase and G6PD, in renal tissue. The increased amount of free amino acid nitrogen in the renal tissue found in the present study also indicates suppression of gluconeogenic mechanisms. Additionally, Cr(VI) increased the transaminase activity and resulted in histopathological changes such as tubular inflammation and degenerative vacuolization of renal tissue. It is well-known that, in mammalian systems, Cr(VI) exposure can induce inflammation in renal tissue that significantly increases the activities GPT and GOT [42]. Transaminase activity might also be increased to neutralize the nephrotoxic effects caused by Cr(VI). Deterioration in renal health was reflected in terms of increased alkaline phosphatase activity [43]. In the present study, this enzyme's activity was significantly elevated due to Cr(VI) toxicity. Histological presentation also denoted hyalinization and disintegration of glomerular architecture, tubular dilatation and tissue necrosis, which further indicates the perturbation of renal health.

Chromium salt is known to cause glycosuria and proteinuria in mice and also induces cellular damage, excessive reactive oxygen species production, DNA damage and inflammatory responses [44, 45]. In the present study, synthesis of tissue protein and important proteases were suppressed in renal tissue due to sub-acute Cr(VI) toxicity. Total protein may have been depleted from renal tissue as a consequence of Cr(VI)-induced proteinuria, whereas protease activities (cathepsin, trypsin and pronase) were decreased due to a scarcity of suitable substrates or enzymatic defects. As Cr(VI) is accountable for protein–protein cross linking, protein-DNA cross binding and retrogressive translational modification, it may affect the compatibility of enzymes' active sites with their ligands thus prevent normal renal function [46]. Trypsin is an important protease that degrades polypeptides and peptones into different amino acids according to the biochemical and physiological requirements of the organism. In the present study, sub-acute exposure to Cr(VI) resulted in a significant decrease in trypsin activity in renal tissue that may result either from the depletion of specific substrates of the enzyme or malformation of the enzyme due to genotoxic structural trans-modification. Pronase and cathepsin are two cellular proteases that are responsible for the breakdown of peptides into small intermediates for utilization in cellular processes such as development and energy production [47]. Here, we noted significant disturbance of the activities of pronase and cathepsin following Cr(VI) intoxication due to functional modification of the enzymes.

Conclusion

Cr(VI) exposure seriously impairs certain renal metabolic processes and cellular uniformity leading to renal tissue damage. It has a negative effect on the kinetics of the cooperative assimilation of carbohydrate and protein metabolism in renal tissue. Additionally, Cr(VI) persistently disrupts cellular bioenergetics via its toxic effects on the TCA cycle and oxidative phosphorylation. Excessive deposition of elemental chromium suggests significant tissue damage promoting altered tissue architecture. The reduction in total protein content in Cr(VI)-treated mice is indicative of severe renal tissue damage that may result from proteinuria. Additionally, the observed decrease in protease activities after chromium intoxication reflects disturbance of the normal protein metabolic machinery in renal tissue. Interstitial inflammation and cellular vacuolization may be correlated with the increased activities of transaminases and LDH during Cr(VI) intoxication. Histopathological observation identified glomerulonephritis and tubular necrosis with cellular vacuolization. Gluconeogenic progression was affected by the decreased activity of G6Pase and G6PD, which concurrently restricts glucose formation. Thus, Cr(VI)-induced sub-acute toxicity disrupts normal renal bioenergetics and metabolic cooperation between important ATP-generating biomolecules in the renal tissue of experimental animals.

Acknowledgements

The authors are grateful to the University Grants Commission, New Delhi, India for providing a Non-NET PhD fellowship, UGC merged scheme to K.S. The authors gratefully acknowledge infrastructural assistance received from the State Biotech Hub, Tripura University.

Conflicts of interest statement

None declared.

References

1. De Flora S, Camoirano A, Micale RT *et al*. Reduction of hexavalent chromium by fasted and fed human gastric fluid. I. Chemical reduction and mitigation of mutagenicity. *Toxicol Appl Pharmacol* 2016; 306: 113–119
2. Kirman CR, Suh M, Hays SM *et al*. Reduction of hexavalent chromium by fasted and fed human gastric fluid. II. Ex vivo gastric reduction modelling. *Toxicol Appl Pharmacol* 2016; 306: 120–133
3. Henson MW, Santo Domingo JW, Kourtev PS *et al*. Metabolic and genomic analysis elucidates strain-level variation in *Microbacterium sp*. isolated from chromate contaminated sediment. *PeerJ* 2015; 3: 1–17
4. Soudani N, Troudi A, Amara IB *et al*. Ameliorating effect of selenium on chromium (VI)-induced oxidative damage in the brain of adult rats. *J Physiol Biochem* 2012; 68: 397–409
5. Mishra SR, Pradhan RP, Prusty BA *et al*. Meteorology drives ambient air quality in a valley: a case of Sukinda chromite mine, one among the ten most polluted areas in the world. *Environ Monit Assess* 2016; 188: 1–7

6. Naz A, Mishra BK, Gupta SK. Human health risk assessment of chromium in drinking water: a case study of sukinda chromite mine, Odisha, India. *Exposure and Health* 2016; 8: 253–264
7. Hegazy R, Salama A, Mansour D *et al*. Renoprotective effect of lactoferrin against chromium-induced acute kidney injury in rats: involvement of IL-18 and IGF-1 inhibition. *Plos One* 2016; 11: 1–18
8. Velma V, Tchounwou PB. Oxidative stress and DNA damage induced by chromium in liver and kidney of goldfish, *Carassius auratus*. *Biomark Insights* 2013; 8: 43–51
9. Dutta M, Bandyopadhyay D, Chattopadhyay A *et al*. Aqueous bark extract of *Terminalia arjuna* protects against high fat diet aggravated arsenic-induced oxidative stress in rat heart and liver, involvement of antioxidant mechanisms. *J Pharm Res* 2014; 8: 1285–1302
10. Krishnaiah C, Reddy KP. Dose-dependent effects of fluoride on neurochemical milieu in the hippocampus and neocortex of rat brain. *Fluoride* 2007; 40: 101–110
11. Segal S, Blair AE, Wyngaarden JB. An enzymatic spectrophotometric method for the determination of pyruvic acid in blood. *J Lab Clin Med* 1956; 48: 137–143
12. Taylor KA. A simple colorimetric assay for muramic acid and lactic acid. *Appl Biochem Biotech* 1996; 56: 49–58
13. Bergmeyer HU. *Methods of Enzymatic Analysis*. Weinheim, Germany: Verlag Chemie, 1983, 204–205
14. Liu XI, Bisswanger H. Solvent isotope effect on the reaction catalysed by the pyruvate dehydrogenase complex from Escherichia coli. *Biol Chem* 2003; 384: 673–679
15. Plummer DT. *An Introduction to Practical Biochemistry*. New Delhi, India: Tata McGraw-Hill Education Pvt. Ltd, 1988, 273
16. Bergmeyer HU. *Methods of Enzymatic Analysis*. Weinheim, Germany: Verlag Chemie, 1983, 232–234
17. King J. *Practical Clinical Enzymology*. London, UK: Nostrand Co., 1965, 121–138
18. Mehler AH, Kornberg A, Grisolia S *et al*. The enzymatic mechanism of oxidation reductions between malate or isocitrate and pyruvate. *J Biol Chem* 1948; 174: 961–977
19. Minakami S, Ringler RL, Singer TP. Studies on the respiratory chain-linked dihydrodiphosphopyridine nucleotide dehydrogenase. Assay of the enzyme in particulate and in soluble preparation. *J Biol Chem* 1962; 237: 569–576
20. Lowry OH, Rosebrough NJ, Farr AL *et al*. Protein measurement with the folin phenol reagent. *J Biol Chem* 1951; 193: 265–275
21. Rosen H. A modified ninhydrin colorimetric analysis for amino acids. *Arch Biochem Biophys* 1957; 67: 10–15
22. Kind PR, King EJ. Estimation of plasma phosphatase by determination of hydrolysed phenol with amino-antipyrine. *J Clin Pathol* 1954; 7: 322–326
23. Reitman S, Frankel S. Determination of serum glutamic oxaloacetic and glutamic pyruvic transaminase. *Am J Clin Pathol* 1957; 28: 56–60
24. Barman TE. *Enzyme Hand Book*. New York, USA: Springer, 1974, 105–110
25. Green NM, Work E. Pancreatic trypsin inhibitor: Reaction with trypsin. *Biochem J* 1953; 54: 347–352
26. Pokrovsky AA, Archakov AI, Lyubimtseva ON *et al*. *Laboratory Manual in Biochemistry*. Moscow: Mir Publisher, 1989, 160–162
27. Sun Z, Liang P. Determination of Cr (III) and total Cr(VI) in water samples by cloud point extraction and flame atomic absorption spectrometry. *Microchim Acta* 2008; 162: 121–125
28. Abreu PL, Ferreira LMR, Urbano AM. Impact of hexavalent chromium on mammalian cell bioenergetics, phenotypic changes, molecular basis and potential relevance to chromate-induced lung cancer. *Biometals* 2014; 27: 409–443
29. Kim SJ, Gil HW, Yang JO *et al*. The clinical features of acute kidney injury in patients with acute paraquat intoxication. *Nephrol Dial Transplant* 2009; 24: 1226–1232
30. Błasiak J, Kowalik J. A comparison of the in vitro genotoxicity of tri-and hexavalent chromium. *Mutat Res Genet Toxicol Environ Mutagen* 2000; 469: 135–145
31. Andersson MA, Grawe KV, Karlsson OM *et al*. Evaluation of the potential genotoxicity of chromium picolinate in mammalian cells in vivo and in vitro. *Food Chem Toxicol* 2007; 45: 1097–1106
32. Bosgelmez II, Soylemezolu T, Guvendik G. The protective and antidotal effects of taurine on hexavalent chromium-induced oxidative stress in mice liver tissue. *Biol Trace Elem Res* 2008; 125: 46–58
33. Sridevi BV, Reddy K, Reddy SL. Effect of trivalent and hexavalent chromium on antioxidant enzyme activities and lipid peroxidation in a freshwater field crab, *Barytelphusa guerini*. *Bull Environ Contam Toxicol* 1998; 63: 384–390
34. Li WJ, Yang CL, Chow KC *et al*. Hexavalent chromium induces expression of mesenchymal and stem cell markers in renal epithelial cells. *Mol Carcinog* 2016; 55: 182–192
35. Zager RA, Johnson AC, Becker K. Renal cortical pyruvate depletion during AKI. *J Am Soc Nephrol* 2014; 25: 998–1012
36. Kleegberg J, Gitelson S. The blood pyruvic acid level in renal diseases and in ureamic coma. *J Clin Pathol* 1956; 9: 148–152
37. Wedeen RP, Qian LF. Chromium-induced kidney disease. *Environ Health Perspect* 1991; 92: 71–74
38. De-Geus HR, Betjes MG, Bakker J. Biomarkers for the prediction of acute kidney injury: a narrative review on current status and future challenges. *Clin Kidney J* 2012; 5: 102–108
39. Garcia-Nino WR, Pedraza-Chaverri J. Protective effect of curcumin against heavy metals-induced liver damage. *Food Chem Toxicol* 2014; 69: 182–201
40. Shil K, Pal S. Hexavalent chromium induced alteration of carbohydrate bioenergetics: a dose-dependent study. *Asian J Pharm Clin Res* 2017; 10: 410–417
41. Trujillo J, Chirino YI, Molina-Jijon E *et al*. Renoprotective effect of the antioxidant curcumin: recent findings. *Redox Biol* 2013; 1: 448–456
42. Balakrishnan R, Kumar CS, Rani MU *et al*. An evaluation of the protective role of α-tocopherol on free radical induced hepatotoxicity and nephrotoxicity due to chromium in rats. *Indian J Pharmacol* 2013; 45: 490–495
43. Damera S, Raphael KL, Baird BC *et al*. Serum alkaline phosphatase levels associate with elevated serum C-reactive protein in chronic kidney disease. *Kidney Int* 2011; 79: 228–233
44. Gwinner W, Gröne HJ. Role of reactive oxygen species in glomerulonephritis. *Nephrol Dial Transplant* 2000; 15: 1127–1132
45. Madejczyk MS, Baer CE, Dennis WE *et al*. Temporal changes in rat liver gene expression after acute cadmium and chromium exposure. *Plos One* 2015; 10: 1–27
46. Molina-Jijon E, Zarco-Marquez G, Medina-Campos ON *et al*. Deferoxamine pretreatment prevents Cr (VI)-induced nephrotoxicity and oxidant stress: role of Cr (VI) chelation. *Toxicology* 2012; 29: 93–101
47. Croall DE, De-Martino GN. Calcium-activated neutral protease (calpain) system: structure, function, and regulation. *Physiol Rev* 1991; 71: 813–847

Clinical Kidney Journal
ckj